HHS Public Access

Author manuscript

Abdom Radiol (NY). Author manuscript; available in PMC 2019 December 19.

Published in final edited form as:

Abdom Radiol (NY). 2018 November ; 43(11): 3117–3124. doi:10.1007/s00261-018-1598-9.

3T Multiparametric MR Imaging, PIRADSv2 Based Detection of Index Prostate Cancer Lesions in the Transition Zone and the Peripheral Zone Using Whole Mount Histopathology as Reference Standard

Nazanin Hajarol Asvadi, MD[1], **Sohrab Afshari Mirak, MD**[1], **Amirhossein Mohammadian Bajgiran, MD**[1], **Pooria Khoshnoodi, MD**[1], **Pornphan Wibulpolprasert, MD**[2], **Anthony Sisk, MD**[3], **Robert Reiter, MD**[4], **Steven S. Raman, MD**[1,4]

[1]Department of Radiological Sciences, David Geffen School of Medicine at UCLA, 757 Westwood Plaza, Los Angeles, CA 90095 [2]Department of Radiology, Ramathibodi Hospital, Bangkok, Thailand [3]Department of Pathology, David Geffen School of Medicine at UCLA, 757 Westwood Plaza, Los Angeles, CA 90095 [4]Department of Urology, David Geffen School of Medicine at UCLA, 757 Westwood Plaza, Los Angeles, CA 90095

Abstract

Purpose: To evaluate 3T mpMRI characteristics of transition zone and peripheral zone index prostate cancer lesions stratified by Gleason Score and PI-RADSv2 with whole mount histopathology correlation.

Methods: An institution review board approved, HIPAA compliant single arm observational study of 425 consecutive men with 3T mpMRI prior to radical prostatectomy from December 2009 to October 2016 was performed. A genitourinary radiologist and a genitourinary pathologist matched all lesions detected on whole mount histopathology with lesions concordant for size and location on 3T mpMRI. Differences in clinical, MRI parameters, and histopathology between transition zone and peripheral zone were determined and analyzed with Chi-square and Mann-Whitney U test. AUC was measured.

Results: 3T mpMRI detected 248/323 (76.7%) index lesions in peripheral zone and 75/323 (23.2%) in transition zone. Transition zone prostate cancer had higher median prostate specific antigen (p=0.001), larger tumor on 3T mpMRI (p=0.001), lower proportions of PI-RADSv2 category 4 and 5 (p<0.001), and lower pathological stage (p=0.055) compared to peripheral zone prostate cancer. No significant differences were detected in prostate specific antigen density, preoperative biopsy and pathology Gleason Scores. After adjusting for significant variables from univariate analysis including prostate volume, tumor volume, prostate specific antigen, PI-

Corresponding Author: Sohrab Afshari Mirak, 757 Westwood Blvd., Los Angeles, CA 90095, Telephone: 310-2065687, Fax: 310-8256201, safsharimirak@mednet.ucla.edu.

Conflict of Interest: The authors declare that they have no conflict of interest.

Ethical approval: This study was performed in accordance with the 1996 Health Information Portability and Accountability Act (HIPAA) and under waiver of informed consent by the institutional review board (IRB).

Consent: For this type of study formal consent is not required

RADSv2 category, AUC for predicting clinically significant tumor in transition zone and peripheral zone were 0.80 and 0.72, respectively (p=0.36).

Conclusions: The diagnostic performance of PI-RADSv2 for clinically significant transition and peripheral zone prostate cancer was similar. However, there was a lower portion of PI-RADSv2 4 and 5 lesions in transition zone compared to peripheral zone.

Keywords

Prostate Cancer; Multi-parametric Magnetic Resonance Imaging; PI-RADSv2; Gleason Score

Introduction

Prostate cancer (PCa) is the second leading cause of cancer-related death of men in the United States [1]. For patients with high clinical suspicion for PCa (abnormal digital rectal exam, elevated serum prostate specific antigen (PSA)), the standard of care for the diagnosis of PCa is systematic transrectal ultrasound (TRUS) guided biopsy [2]. Multi-parametric prostate MRI (mpMRI) using T2 weighted imaging (T2WI), diffusion weighted imaging (DWI), and dynamic contrast enhancement (DCE) has allowed for characterization of prostate cancer [3–5]. Although the different characteristics of transition zone (TZ) and peripheral zone (PZ) PCa with mpMRI has been reported [6–9], a robust subanalysis in a large cohort stratified by zonal anatomy has not been extensively studied. Generally, previous studies have paid much attention to demonstrate different characteristics of PCa lesions located in PZ rather than TZ. TZ lesions have overlapping imaging features with benign lesions such as benign prostatic hyperplasia (BPH) and they have reportedly different pathological and clinical characteristics from PZ lesions [10]. The most recent version of the Prostate Imaging – Reporting and Data System version 2 (PI-RADSv2) is a consensus based document that has different imaging criteria for TZ and PZ lesions [11]. The purpose of this study was to evaluate different clinical and imaging characteristics of the index TZ compared to index PZ PCa on 3T mpMRI stratified by Gleason Score (GS) and PI-RADSv2 with of whole mount histopathology (WMHP) as a reference standard.

Materials and Methods

Study Population

This study was performed in accordance with the 1996 Health Information Portability and Accountability Act (HIPAA) and under waiver of informed consent by the institutional review board (IRB). This retrospective study cohort included 425 consecutive men who underwent 3T mpMRI for suspected PCa followed by robotic assisted radical prostatectomy (RALP) between December 2009 and October 2016. All patients underwent 3T mpMRI for PCa detection, grading and staging prior to RALP. All index lesions were included in the study. Index lesion was defined as the tumor with the highest grade, and/or the largest lesion if more than one PCa lesion had the same GS. Exclusion criteria were patients with prior radiation therapy or prostate resection, contraindication for MRI and technical limitations including artifact.

MRI Imaging protocol and interpretation

All men in this cohort underwent preoperative 3T mpMRI on one of several 3T systems (Siemens Magnetom Trio, Skyra or Verio scanners (Siemens Medical Systems, Malvern, Pennsylvania, USA)) using similar protocols and with pelvic external phased array coils and endorectal coil (See Table 1 for MRI protocol). Patients were given 1mg of an anti-peristaltic agent (glucagon (Glucagen, Lilly, In, USA)) intramuscularly to reduce bowel peristalsis. DCE protocol involved injection with 0.1 mg/kg Gadopentetate Dimeglumine (Magnevist, Bayer), administered at 2 mL/s at the second acquisition for baseline calculation. The study was then transferred to a separate workstation (DynaCAD, InVivo Inc., Gainesville, FL) for processing of the DWI and DCE images for image interpretation. (Figure 1 and 2)

Each 3T mpMRI study was interpreted by an abdominal imaging fellow (postgraduate year 6) and one of three board-certified abdominal imaging radiologists with 22 (DSKL), 18 (SSR) and 13 (DJAM) years of experience in interpreting prostate MR Imaging. Each AI radiologist interpreted the study using T2WI, T1WI, calculated high b-value DWI (b=1400), average Apparent Diffusion Coefficient (ADC) mapping of the most characteristic sub-area of the tumor, which derived from a separate DWI imaging from five evenly spaced b values ranging from 0 to 800 sec/mm2 and DCE imaging including dynamic assessment of enhancement as well as calculation of pharmacokinetic parameters in suspected lesions. Each individual lesion was identified and localized within the prostate and assigned a PI-RADSv2 score. The individual and overall PI-RADSv2 categories are determined by the following factors: DWI, T2WI and DCE appearances based on PI-RADSv2 [12].One genitourinary (GU) radiologists ((PW) 6 years experience) read the pre-procedure diagnostic MRI independently which had access to clinical information but not the biopsy results and provided PI-RADSv2 category retrospectively.

Pathology

Each prostatectomy was sectioned at approximately 5mm intervals in an axial plane using WMHP technique as standard of care. One of three experienced GU pathologists interpreted each study blinded to all MR information and determined the size, GS and location (apex, midgland, base), invasiveness (extracapsular extension or seminal vesicle invasion) and stage of each PCa lesion independent of MRI results. Each section was photographed and each whole mount slide was scanned for inclusion in our database. The GU pathologists had access to clinical information (PSA and prior biopsy results) at the time of pathological review as part of standard clinical practice. PI-RADSv2 sector mapping was used to categorize the location of each lesion (TZ and PZ) in WMHP. (Figure 1 and 2).

Correlation of mpMRI and WMHP

At a monthly joint radiology-pathology meeting, the WMHP sections were reviewed, and correlated with mpMRI sections by the GU pathologists and GU radiologists (DJAM). Each PCa lesion identified on WMHP was outlined on each section and classified as true positive if present or false negative if absent on the most closely corresponding mpMRI section. Lesions detected on mpMRI without a correlate on WMHP were classified as false positive. The tumor diameter of each PCa lesion on mpMRI was measured on axial T2W image and

confirmed on ADC and if true positive, was compared to the tumor diameter measured on WMHP based on maximum diameter of the tumor.

Patient Data

A number of the following variables were compiled into our database: clinical (age, PSA, postoperative follow up), 3T mpMRI (MR lesion diameter, average ADC, endorectal coil employment, prostate volume, tumor volume, prostate zone, PI-RADSv2 category, radiologist) and pathological (prior TRUS or MR fusion biopsy GS, number of cores positive, percentage of cores positive, prostate weight, GS, PCa staging, tumor diameter, positive surgical margins). We used prostate weight in our evaluations as it correlates closely with prostate volume [13]. Prostate capsule and the lesion were manually contoured on T2WI and the volumes were calculated with Profuse software (Eigen, Grass Valley, California). PSA density was defined as pre-operative PSA divided by MRI prostate volume. Clinically significant PCa was defined as GS ≥7 (≥ 3+4), independent of tumor size and only index lesions were included in this study. Patients were followed postoperatively for a median period of 16 months.

Statistical Analysis

For continuous variables, we reported the median and interquartile range (IQR). Differences in clinical, MRI parameters and histopathology between TZ and PZ lesions were determined. In addition, the differences between false positives (FP) lesions in mpMRI in TZ and PZ and the difference between false negatives (FN) lesions on pathology were reported. Differences in categorical variables were evaluated using Fisher or chi-squared tests and for continuous variables were calculated using non-parametric Mann-Whitney U test. Linear logistic regression and subsequent area under the curve (AUC) were used for tumor detection on mpMRI for TZ, PZ and for the whole prostate using WMHP findings as the reference standard. All statistical analyses were performed using STATA 12.1. A p-value <0.05 was considered significant. We did not correct for multi-testing because planned comparisons were used.

Results

A total of 425 patients with median age of 62.1 years (IQR 56.8–67.5) and median PSA of 6.0 (IQR 4.6–8.2) ng/ml were included in the study. Table 2 shows patients' demographic, MRI and pathology related information. Of the 425 index lesions, 3T mpMRI detected the index lesion in 323 (76.0%). In this cohort, 62.8% (267/425) underwent mpMRI with an endorectal coil. Ten of 425 (2.3%) patients scheduled for 3T underwent 1.5 T mpMRI due to implanted hardware or pacemakers and were excluded from the lesion-level analysis. Of the 425 patients, 259 (60.9%) had post-op PSA and 206 of 259 (79.5%) patients with post-op PSA also had 3T mpMRI visualized index lesions; 53/259 (20.5%) patients with post-op PSA and without index lesions detected by mpMRI were excluded from zone-level analysis. Median time between 3T mpMRI and surgery was 55.0 (IQR 21.0–98.0) days. Median number of lesions was 2.0 (IQR 1.0–3.0). Median 3T mpMRI prostate volume was 35.8 (IQR 25–46) cm^3 and median 3T mpMRI tumor volume was 0.35 (IQR 0.17–0.92) cm^3. Median prostate weight on pathology was 42.0 (IQR 34.0–54.0) gm. There was a strong

correlation between estimated MRI prostate volume and pathologically measured prostate weight (r=0.850 (p <0.001)) (Figure 3). Overall, 45.5% (147/323) and 32.5% (105/323) of all index lesions were scored PI-RADSv2 category 4 and 5, respectively. Most patients (99.1% (421/425)) had a preoperative core needle biopsy (TRUS 66.8% (284/425), MR-US fusion 31.7% (135/425) and MR-guided biopsy 0.7% (3/425)), with the majority of the lesions being diagnosed as GS 3+3 (27.1% (115/425)) and GS 3+4 (37.4% (159/425)). Most patients had Stage 2 PCa (66.3% (282/425)) and 363/425 (85.4%) of the PCa lesions on WMHP were clinically significant. Median follow up time was 16 months (IQR 4.6–29.0 months).

Table 3 shows different clinical, MRI and pathology characteristics of true positive index lesions in TZ and PZ and compares them between two groups. 3T mpMRI detected 75/323 (23.2%) and 248/323 (76.7%) index lesions in TZ and PZ, respectively. Compared to patients with PZ PCa, patients with TZ PCa had higher PSA (median 7.7 vs. 5.9 ng/ml, p=0.001), higher pathological tumor diameter (2.4 vs 2.0 cm, p=0.003) and higher tumor volume (0.52 vs. 0.30 cm^3, p=0.001), lower proportions of mpMRI PI-RADS category 4 and 5 (65.8% vs 81.4%, p<0.001) with slightly lower portion of pathological stage 3b (2.7% vs 11.7%, p=0.055). There were no significant differences in other variables between patients with TZ and PZ PCa including: 3T mpMRI prostate volume (39.9 vs. 35 cm^3, p=0.155), and pathology prostate weight (41.5 vs. 42.0 gm, p=0.8), PSA density (0.18 vs. 0.17 ng/ml/cc, p=0.064), proportion of GS 3+3 (12% vs 8.5%, p=0.317), biopsy GS (p=0.386), and surgical margin positivity (p=0.83). After adjusting for significant variables from univariate analysis including prostate volume and tumor volume on MRI, PSA, PI-RADSv2 category, the AUC for TZ was 0.80 compared to PZ 0.72 for predicting clinically significant PCa compared to low grade tumor (p=0.36) (See Figure 4).

Table 4 shows different characteristics of FN and FP PCa index lesions in TZ and PZ and compares them between two groups. There were significant differences between FP index lesions in TZ and PZ in prostate volume on mpMRI (p=0.021) and PI-RADSv2 category (p=0.033). TZ PCa lesion tended to be in larger prostates with higher proportion of PI-RADSv2 scores 2 and 3, as compared to PZ PCa lesions with higher rate of PI-RADSv2 scores 3 and 4. However, no significant difference in mpMRI tumor volume was detected (p=0.5). There were no significant difference between FN index lesions in TZ and PZ in pathology tumor diameter (p=0.176), biopsy GS (p=0.595), pathology GS (p=0.298), and pathology staging (p=0.488).

Discussion

To our knowledge, this is the first and largest study with WMHP standard to demonstrate 3T mpMRI is able to reliably image differences in PCa characteristics in the TZ and PZ, previously reported pathologically. Patients with TZ PCa had higher serum PSA, larger PCa volume, and had more favorable pathological staging after radical prostatectomy compared to patients with PZ PCa, as reported previously in studies based on pathology [14,15]. We reported that the median PCa volume in the TZ on 3T mpMRI was 1.5 times larger than PZ PCa measured on T2WI in both zones, radiologically mirroring results by Lee [14] who reported a twofold increase in pathological tumor volumes in the TZ compared to PZ.

Overall, we demonstrated a concordant difference between the prostate volume on 3T mpMRI and prostate weight on surgical pathology. The significantly higher PCa volume in the TZ likely results in the higher PSA that we and others have reported for patients with TZ PCa compared to PZ PCa [14]. The median PSA increase in patients with TZ lesions was proportional to the median PCa volume increase. In contrast, older studies such as Noguchi et al [15] did not report a difference in preoperative PSA or GS in the two groups likely because their patient population included more advanced disease in PZ PCa in the pre-PSA era with a significantly higher proportion of higher risk disease compared to more contemporary post-PSA era cohorts reported by Lee et al and the present study.

We also reported for the first time in a large cohort that there is lower portion of PI-RADSv2 score 4 or higher in TZ compared to PZ index lesions which may be in part due to less aggressive biology of TZ lesions as it was demonstrated with prior pathological studies [10]. However, another explanation might be the presence of features such as benign prostatic hyperplasia nodules in TZ that can mimic PCa and will result in the reader's less confidence in diagnosing tumor as well. Despite these differences, the diagnostic performance of PI-RADSv2 was similar in the TZ compared to PZ. Muller et al [16] study evaluated 88 biopsy proven PCa lesions in 94 patients and reported slightly better performance of revised PI-RADSv2 for detection of TZ tumor (AUC 0.87) compared to PZ tumors (AUC 0.86), comparable to our results in the TZ (AUC 0.80) and PZ (AUC 0.72) in a larger cohort with a much more robust WMHP as the standard of reference. In another study, using 3T in bore MR guided targeted biopsy results as the reference standard; there was a similarly improved diagnostic performance in the TZ over PZ using PI-RADSv2 [9]. Rosenkrantz et al [11] reported slightly lower interobserver agreement for PI-RADSv2 score of 4 or higher in the TZ compared to the PZ. However, there was an improvement in PI-RADSv2 compared to PI-RADSv1. The improved performance of PI-RADSv2 in the TZ may also be in part due to the emphasis on T2 weighted imaging for TZ tumors in contrast to DWI for PZ lesions. Furthermore, there was also a significant difference between FP index lesions in PI-RADSv2 category in TZ and PZ.

There are several limitations to the study. First, it is subject to selection and verification bias given a WMHP reference standard. Second, we only selected patients who underwent robotic prostatectomy and low risk patients who were active surveillance candidates were not included and therefore, further study will be needed to determine if results can be applied to an active surveillance population. However, the Muller and Tan studies with a targeted biopsy reference standard also seem to corroborate our results. Third, this single institutional tertiary center experience with subspecialty expertise in urological oncology, GU radiology, MR Imaging and pathology may not be generalizable to all practices. Fourth, we only included index lesions. Therefore, further studies are required to compare the index and satellite tumors in the TZ and the PZ. Fifth, interreader agreement was not determined in this study.

In conclusion, in this study we demonstrated that, compared to PZ PCa, TZ PCa has significantly higher PSA and tumor volume on 3T mpMRI similar to prior pathological studies. Despite the larger tumor volume, we demonstrated favorable pathological staging for TZ PCa compared to PZ PCa. Concordant with imaging characteristics of TZ PCa, we

have also shown similar diagnostic performance of PI-RADSv2 in diagnosing clinically significant PCa for TZ PCa compared to PZ PCa similar to prior smaller studies, and lower portion of PI-RADSv2 of 4 and 5 likely reflecting more favorable tumor biology of TZ lesions. Using PI-RADSv2, 3T mpMRI may help elucidate the histopathological differences between TZ and PZ PCa and further improve risk stratification of patients with PCa for surgical triage. Further study will be necessary to determine if this can be applied to active surveillance and other populations.

Acknowledgement:

We are grateful to Mark DeMars, William Hsu, Wenchao Tao, Cleo Maehara who support our research. Statistical analyses for this research were supported by NIH National Center for Advancing Translational Science (NCATS) UCLA CTSI Grant Number UL1TR001881. We are also thankful to Tristan R. Grogan for his statistical analyses support.

Financial Disclosure: The study was supported in part by the department of Radiology and Pathology Integrated Diagnostics (IDx) program and specialized program of research excellence (SPORE) of PCa.

References

1. Key statistics for prostate cancer. (2015). http://www.cancer.org/cancer/prostatecancer/detailedguide/prostate-cancer-key-statistics. Accessed 4/29/2016 2016
2. Early Detection of Prostate Cancer: AUA Guidelines. https://www.auanet.org/education/guidelines/prostate-cancer-detection.cfm. Accessed 4/28/2016 2016
3. Haider MA, van der Kwast TH, Tanguay J, Evans AJ, Hashmi AT, Lockwood G, Trachtenberg J (2007) Combined T2-weighted and diffusion-weighted MRI for localization of prostate cancer. AJR Am J Roentgenol 189 (2):323–328. doi:10.2214/ajr.07.2211 [PubMed: 17646457]
4. Engelbrecht MR, Huisman HJ, Laheij RJ, Jager GJ, van Leenders GJ, Hulsbergen-Van De Kaa CA, de la Rosette JJ, Blickman JG, Barentsz JO (2003) Discrimination of prostate cancer from normal peripheral zone and central gland tissue by using dynamic contrast-enhanced MR imaging. Radiology 229 (1):248–254. doi:10.1148/radiol.2291020200 [PubMed: 12944607]
5. Le JD, Tan N, Shkolyar E, Lu DY, Kwan L, Marks LS, Huang J, Margolis DJ, Raman SS, Reiter RE (2015) Multifocality and prostate cancer detection by multiparametric magnetic resonance imaging: correlation with whole-mount histopathology. Eur Urol 67 (3):569–576. doi:10.1016/j.eururo.2014.08.079 [PubMed: 25257029]
6. Delongchamps NB, Rouanne M, Flam T, Beuvon F, Liberatore M, Zerbib M, Cornud F (2011) Multiparametric magnetic resonance imaging for the detection and localization of prostate cancer: combination of T2-weighted, dynamic contrast-enhanced and diffusion-weighted imaging. BJU Int 107 (9):1411–1418. doi:10.1111/j.1464-410X.2010.09808.x [PubMed: 21044250]
7. Hoeks CM, Hambrock T, Yakar D, Hulsbergen-van de Kaa CA, Feuth T, Witjes JA, Futterer JJ, Barentsz JO (2013) Transition zone prostate cancer: detection and localization with 3-T multiparametric MR imaging. Radiology 266 (1):207–217. doi:10.1148/radiol.12120281 [PubMed: 23143029]
8. Vos EK, Kobus T, Litjens GJ, Hambrock T, Hulsbergen-van de Kaa CA, Barentsz JO, Maas MC, Scheenen TW (2015) Multiparametric Magnetic Resonance Imaging for Discriminating Low-Grade From High-Grade Prostate Cancer. Invest Radiol 50 (8):490–497. doi:10.1097/rli.0000000000000157 [PubMed: 25867656]
9. Tan N, Lin WC, Khoshnoodi P, Asvadi NH, Yoshida J, Margolis DJ, Lu DS, Wu H, Sung KH, Lu DY, Huang J, Raman SS (2016) In-Bore 3-T MR-guided Transrectal Targeted Prostate Biopsy: Prostate Imaging Reporting and Data System Version 2-based Diagnostic Performance for Detection of Prostate Cancer. Radiology:152827. doi:10.1148/radiol.2016152827
10. Garcia JJ, Al-Ahmadie HA, Gopalan A, Tickoo SK, Scardino PT, Reuter VE, Fine SW (2008) Do prostatic transition zone tumors have a distinct morphology? Am J Surg Pathol 32 (11):1709–1714. doi:10.1097/PAS.0b013e318172ee97 [PubMed: 18769336]

11. Rosenkrantz AB, Ginocchio LA, Cornfeld D, Froemming AT, Gupta RT, Turkbey B, Westphalen AC, Babb JS, Margolis DJ (2016) Interobserver reproducibility of the PI-RADS version 2 Lexicon: a multicenter study of six experienced prostate radiologists. Radiology:152542
12. American College of R PIRADS v2. Reston, Va: American College of Radiology, 2014.
13. Varma M, Morgan JM (2010) The weight of the prostate gland is an excellent surrogate for gland volume. Histopathology 57 (1):55–58. doi:10.1111/j.1365-2559.2010.03591.x [PubMed: 20653780]
14. Lee JJ, Thomas IC, Nolley R, Ferrari M, Brooks JD, Leppert JT (2015) Biologic differences between peripheral and transition zone prostate cancer. Prostate 75 (2):183–190. doi:10.1002/pros.22903 [PubMed: 25327466]
15. Noguchi M, Stamey TA, Neal JE, Yemoto CE (2000) An analysis of 148 consecutive transition zone cancers: clinical and histological characteristics. J Urol 163 (6):1751–1755 [PubMed: 10799175]
16. Muller BG, Shih JH, Sankineni S, Marko J, Rais-Bahrami S, George AK, de la Rosette JJ, Merino MJ, Wood BJ, Pinto P, Choyke PL, Turkbey B (2015) Prostate Cancer: Interobserver Agreement and Accuracy with the Revised Prostate Imaging Reporting and Data System at Multiparametric MR Imaging. Radiology 277 (3):741–750. doi:10.1148/radiol.2015142818 [PubMed: 26098458]

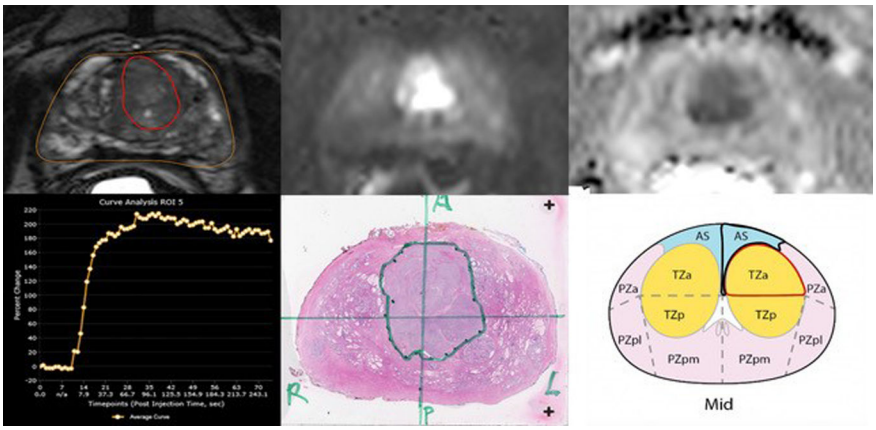

Fig. 1.

Multiparametric 3T MRI in a 58-year-old man with a history biopsy-proven PCa with PI-RADSv2 score of 5. (a) Axial T2-weighted MR image show transition zone lesion with 2.92 cm^3 (b) DWI shows focal high intensity (c) ADC map shows focal low intensity (d) DCE curve shows early and intense enhancement with washout. (e) Wholemount histopathology with maximum tumor diameter of 2.5 cm, GS 4+4 and tumor stage T2C (f) PI-RADSv2 sector map

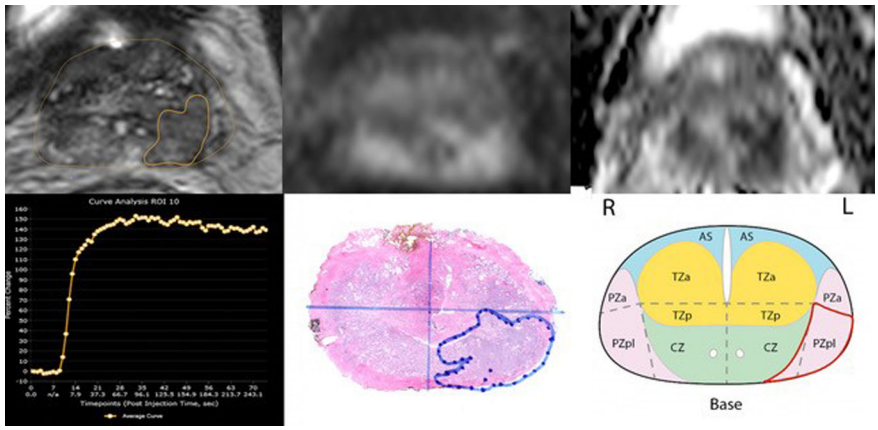

Fig. 2.

Multiparametric 3T MRI in a 66-year-old man with a history biopsy-proven PCa with PI-RADSv2 score of 4. (a) Axial T2-weighted MR image show peripheral zone lesion with 0.26 cm^3 (b) DWI shows focal high intensity (c) ADC map shows focal low intensity (d) DCE curve shows early and intense enhancement with immediate washout (e) Wholemount histopathology with maximum tumor diameter of 2 cm, GS 3+4 and tumor stage T2 (f) PI-RADSv2 sector map

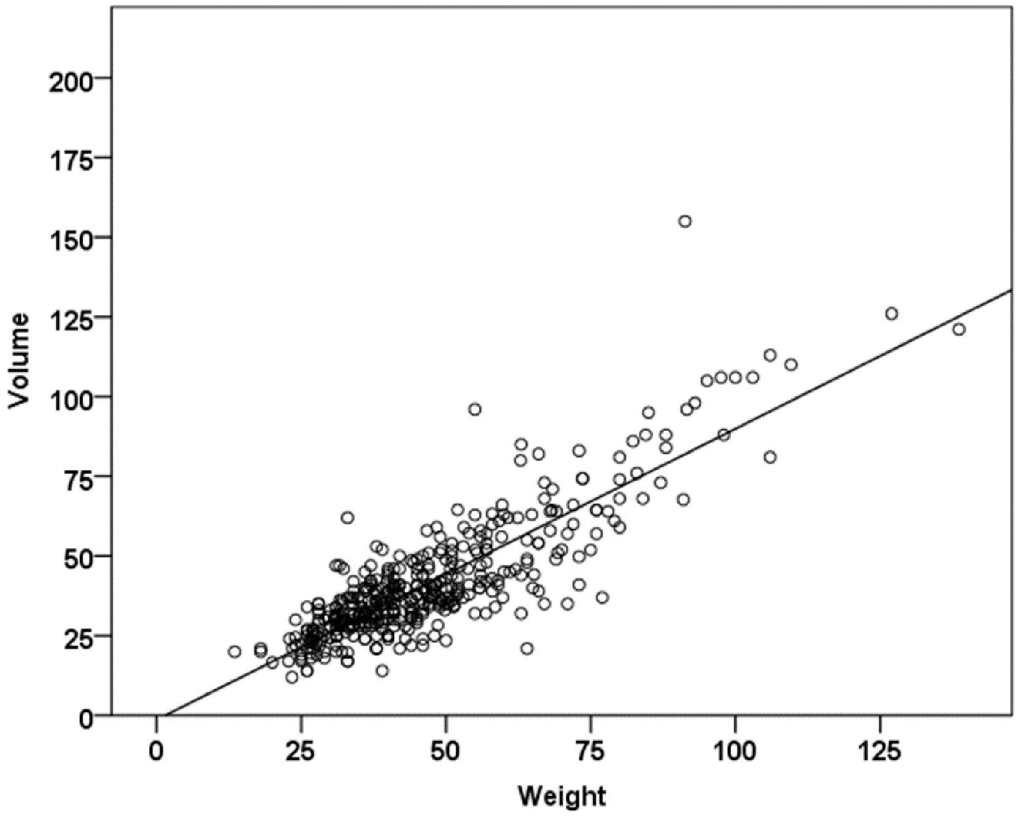

Fig. 3.
Scatterplot and correlation analysis for pathology prostate weight and MRI prostate volume

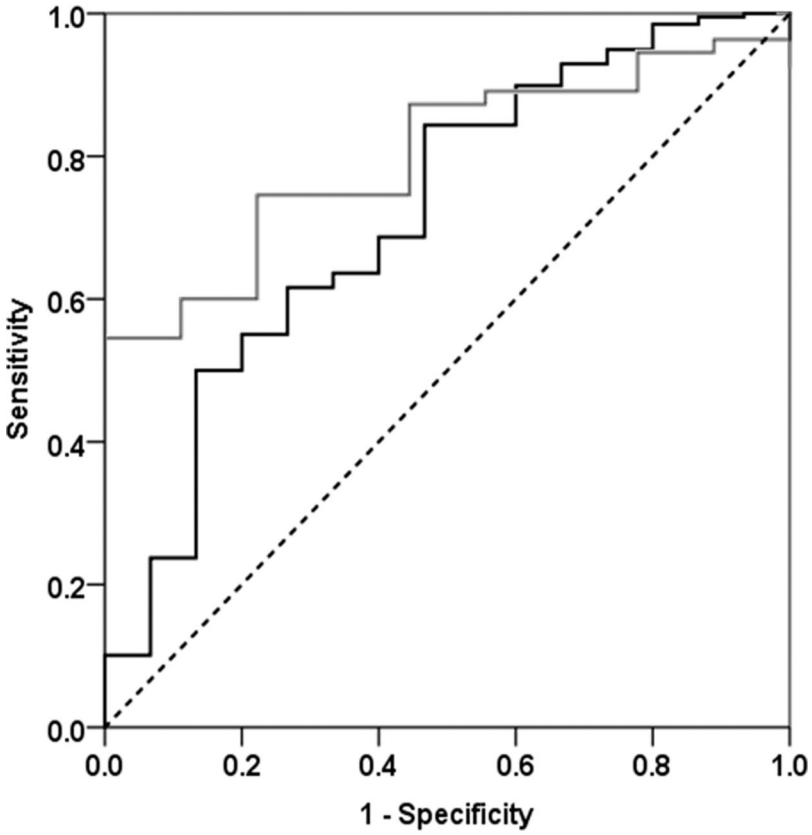

Fig. 4.
AUC for PI-RADSv2 detection of TZ and PZ PCa on 3T mpMRI after adjusting for significant variables

Table 1.

MRI Protocol

Sequence	Repetition Time (ms)	Echo time (ms)	Acquisition Time	Flip angle (degrees)	Slice thickness (mm)	FOV (mm)	Matrix size	averages	B-value (s/mm^2)	Temporal Resolution (s)
3D T2 Turbo-spin Echo (TSE)	2200	202	4:10	110	1.5	210 × 210	225 × 230	2	--	--
Diffusion Weighted Imaging (DWI) Echo Planar	4600	99	5:50	EPI	3.6	210 × 260	160 × 94	8	0, 100, 400, 800, calculated 1400	
Dynamic Contrast Enhancement (DCE) 3D Gradient	4.23	1.46	6:00	12	3.6	260 × 260	259 × 192	1		4.75 s

Table 2.

Patient Demographics

Variable	N (%)
# patients	425
PSA[a] (ng/ml), median (IQR[b])	6.0 (4.6 – 8.2)
Age (years), median (IQR)	62.1 (56.8–67.5)
3T MRI	415/425 (97.6)
Endorectal coil	267/425 (62.8)
Biopsy Gleason Score, n= 425	425
Missing	4/425 (0.94)
3+3	115/425 (27.1)
3+4	159/425 (37.4)
4+3	44/425 (10.3)
8–10	103/425 (24.2)
PI-RADS[c] category (index lesion), n=425 (%)	
Not detected by MRI[d] (missed)	102/425 (24.0)
2	13/425 (3.1)
3	58/425 (13.6)
4	147/425 (34.6)
5	105/425 (24.7)
MRI tumor volume (cm^3), median (IQR), n=285	0.35 (0.17–0.92)
MRI prostate volume (cm^3), median (IQR)	35.8 (25–46)
MRI Dominant Location, n=323 (%)	
Peripheral Zone, n=244	244/323 (75.5)
Transition zone, n=79	79/323 (24.5)
WMHP[e] index Gleason score, n=425	425
3+3	62/425 (14.6)
3+4	198/425 (46.6)
4+3	51/425 (12.0)
8–10	114/425 (26.8)
Pathology prostate weight (gm), median (IQR)	42.0 (34.0–54.0)
Pathology Stage, n=425	425
2	282/425 (66.3)
3a	112/425 (26.3)
3b	31/425 (7.3)
Post-operative PSA follow up (months), median (IQR)	16 (4.6–29.0)

[a] Prostate Specific Antigen,

[b] Interquartile Range,

[c] Prostate Imaging – Reporting and Data System,

[d] Magnetic Resonance Imaging,

[e] whole mount histopathology

Table 3.

Differences in mpMRI and pathology characteristic between TZ and PZ PCa index lesions detected by mpMRI.

Clinical characteristics	Peripheral zone, (n=248)	Transition zone, (n=75)	P value
PSA[a] (ng/ml), median (IQR[b])	5.90 (4.50 – 8.15)	7.70 (5.30 – 12.10)	0.001
PSA density (ng/ml/cc), median (IQR)	0.17 (0.12 – 0.23)	0.18 (0.13 – 0.31)	0.064
Prostate volume (cm^3), median (IQR)	35.00 (28.30 – 44.20)	39.90 (31.00 – 47.00)	0.155
Biopsy Gleason			
3+3	59 (24.2%)	14 (18.7%)	
3+4	85 (34.8%)	33 (44.0%)	0.386
4+3	31 (12.7%)	6 (8.0%)	
Others	73 (29.4%)	22 (29.3%)	
mpMRI tumor volume (cm^3), median (IQR)	0.30 (0.16 – 0.71)	0.52 (0.25 – 1.74)	0.001
PI-RADSv2[c] category			
2	13 (5.26%)	1 (1.37%)	
3	33 (13.36%)	24 (32.88%)	<0.001
4	133 (53.85%)	16 (21.92%)	
5	68 (27.53%)	32 (43.84%)	
Pathology diameter (cm), median (IQR)	2.00 (1.50 – 2.80)	2.40 (1.90 – 3.40)	0.003
Pathology prostate weight (gm), median (IQR)	42.00 (34.00 – 52.00)	41.45 (33.30 – 51.40)	0.801
Pathology Gleason score			
3+3	21 (8.47%)	9 (12.00%)	
3+4	126 (50.81%)	44 (58.67%)	0.317
4+3	64 (25.81%)	13 (17.33%)	
Others	37 (14.92%)	9 (12.00%)	
Pathology Staging			
2	143 (57.7%)	48 (64.0%)	0.055
3a	76 (30.65%)	25 (33.33%)	
3b	29 (11.69%)	2 (2.67%)	
Positive Surgical Margins	34 (13.7%)	11 (14.7%)	0.834

[a]Prostate Specific Antigen,

[b]Interquartile Range,

[c]Prostate Imaging – Reporting and Data System version 2

Table 4.

Differences in mpMRI and pathology characteristic of TZ and PZ PCa in false negative and false positive index lesions.

Pathology characteristics	**FN[a] PZ[b] (n=73)**	**FN TZ[c] (n=29)**	**P value**
Biopsy Gleason,			
3 +3,	26 (35.6%)	13 (44.8%)	
3+4,	30 (41.1%)	12 (41.4%)	0.595
4+3,	4 (5.5%)	2 (6.9%)	
Others	13 (17.8%)	2 (6.9%)	
Pathology tumor diameter (cm), median (IQR[d])	1.40 (0.80–2.00)	1.60 (1.05–2.60)	0.176
Pathology prostate weight (gm), median (IQR)	49.5 (36.3–71.8)	41.9 (32.6–61)	0.222
Pathology Gleason score			
3 +3,	19 (26%)	9 (31%)	
3+4,	41 (56.2%)	15 (51.7%)	0.298
4+3,	7 (9.6%)	5 (17.2%)	
Others,	6 (8.2%)	0 (0%)	
Pathology Staging			
2,	66 (90.4%)	25 (86.2%)	0.488
3a,	7 (9.6%)	4 (13.8%)	
3b,	0 (0%)	0 (0%)	
mpMRI characteristics	**FP[e] PZ (n=72)**	**FP TZ (n=38)**	**P value**
Prostate volume (cm^3), median (IQR)	37.0 (30.4–48.9)	49.8 (35.0–62.9)	0.021
MRI[f] tumor volume (cm^3), median (IQR)	0.18 (0.07–0.40)	0.23 (0.09–0.38)	0.519
PI-RADSv2[g] category			
2,	13 (18.1%)	15 (39.5%)	0.033
3,	34 (47.2%)	18 (47.4%)	
4,	20 (27.8%)	4 (10.5%)	
5,	5 (6.9%)	1 (2.6%)	

[a] False Negative,

[b] Peripheral Zone,

[c] Transition Zone,

[d] Interquartile Range,

[e] False Positive,

[f] Magnetic Resonance Imaging,

[g] Prostate Imaging – Reporting and Data System version 2